

Finite Element Method analysis application in identifying the causes of brake disc failure

ARTICLE INFO

Received: 2 June 2023
Revised: 7 September 2023
Accepted: 1 December 2023
Available online: 11 January 2024

This article presents the results of brake disc tests aimed at identifying the causes of its failure. The first part of the article presents an analysis of the damageability of selected vehicle components, which showed that among the reported failures, the most failure was the braking system. The assessment of the brake disc worn "properly" as a result of the operation and the deformed brake disc after a very short period of operation was the subject of further analysis. The next part of the article presents issues related to the modeling of thermal loads, and then, trying to assess and search for the cause of abnormal wear of the brake system element, the use of the Finite Element Method. The results of FEM calculations for the cast iron disc confirmed the deformation of the brake disc. This phenomenon had a similar character and course in the FEM analysis as in the real object. In the final part of the article, conclusions and directions for further work were formulated.

Key words: brake disc, deformation measurements, thermal loads, FEM numerical analysis

This is an open access article under the CC BY license (<http://creativecommons.org/licenses/by/4.0/>)

1. Introduction

An important factor for car safety is an effective and reliable braking system. Vehicle manufacturers are intensively working on improving the brakes, with the main aim of improving the durability of brake system components, increasing braking efficiency and resistance to changing temperatures, and shortening the braking distance. An extremely important issue is to increase the resistance to overloads occurring, especially during intensive and long-term braking [1].

The friction brake is a mechanism in which mechanical energy is converted into thermal energy. Thermal processes inseparably accompany the operation of brakes, significantly affecting their functioning and effectiveness. Temperature has a fundamental influence on the course of tribological phenomena on friction surfaces. As the temperature increases, the coefficient of friction changes; as a rule, it initially increases slightly and, at higher temperatures, decreases significantly. This often results in the so-called "fading", i.e. a decrease in braking efficiency at elevated temperatures. In addition, the resistance of the friction pair to abrasive wear decreases. The increase in temperature combined with the phenomenon of thermal expansion causes the occurrence of stresses that are sometimes the source of micro-cracks or deformation of the surface of the brake disc or drum. Therefore, thermal deformations may also be the cause of temporary disturbances in the functioning of the braking system, related to geometric irregularities in the cooperation of friction pairs. It follows from the above that the thermal state of the brakes can significantly affect the braking efficiency, as well as the directional stability of the braked vehicle, which means that this issue is directly related to safety [1, 9].

Conducting tests of braking systems comes down to cyclical inspections at diagnostic stations, and post-exploitation tests are usually related to the observation and analysis of the causes of damage or wear of cooperating elements. Therefore, it is extremely important to develop

research methods that allow for approximate mapping of the process of cooperation of friction elements, including numerical methods. Currently, many methods are used to simulate the cooperation process, starting from mapping the contact of friction elements, including the use of thermal phenomena [2, 3, 7, 12, 14, 21, 26]. As a result of vehicle operation, abnormal wear of the actuators of the braking system, in particular brake discs, often occurs. In addition to the indicated numerical methods of problem analysis, macro- and micro-structural tests of brake discs are also carried out in order to determine the causes of abnormal wear [29]. Due to the significant importance of the risk in terms of reducing, but also environmental protection, e.g. in relation to emissions released as a result of friction, in many drives around the world that actuate the braking system, including brake disc-pad friction devices brake. An example may be the works in which the authors [4, 5, 16, 23, 24] investigate the influence of various friction materials on the brake disc during operation. Included are papers [6] that cover the effects of other factors, such as moisture and corrosion, on friction functions and different brake disc materials.

In this article, trying to make an assessment and looking for the cause of abnormal wear of the brake system element, the use of numerical calculation methods was proposed.

2. Analysis of defectiveness of selected vehicle elements

On the example of service repair orders from a period of one year, an analysis of the damageability of selected vehicle components was carried out. The analysis showed that among the reported malfunctions, the most emergency was the braking system. In the analyzed period, 935 braking system repairs were carried out, compared to 3624 of all repair works. Based on the detailed analyzes and observations, a characteristic element of the braking system, i.e. the damaged brake disc, was selected for further research. This

damage, which was initially identified, consisted of an axial deformation that occurred after a short period of vehicle operation. Due to the deformation of the brake disc, strong vibrations were transmitted to the steering wheel during braking, which indicated a problem and obviously affected safety. Therefore, in order to identify and attempt to determine the cause of brake disc deformation, a strength analysis was carried out using the Finite Element Method. The results of this analysis are presented in section 9.

3. Vehicle braking

The value of the kinetic energy that any moving vehicle achieves depends on the mass of the vehicle and its speed squared. The basic task of the braking system is to reduce the speed of the vehicle until it is effectively stopped and, in terms of energy, to reduce the kinetic energy of the vehicle and convert it through friction into thermal energy. This process is carried out mainly by friction forces resulting from the interaction of interacting executive elements, e.g. brake disc – brake pads or brake drum – brake shoes.

An important element during the braking process is that when the clutch is engaged, then, in addition to the weight of the vehicle, all moving parts of the engine and driveline must be braked. While during low-intensity braking, you can use engine braking (with the throttle closed), during emergency braking, the proper effect can only be obtained when the clutch is disengaged.

All forces acting on the vehicle must be transferred through the contact patch of the tires with the road surface. The maximum value of the resultant longitudinal and lateral reactions is determined by the force on the wheels and the coefficient of adhesion. Each braking system solution is designed to ensure vehicle stability during intensive braking and guarantee the shortest possible braking distance. For the optimization process, it is necessary to know what maximum braking forces for a given vehicle can be transmitted by the front and rear wheels. The answer to this question is the parabola of the ideal distribution of braking forces, which describes the distribution of maximum traction forces that can be obtained by the front and rear wheels of the vehicle during acceleration and braking. In the literature, one can find an approach that allows one to carry out dynamic simulations. They then take into account both the thermal effect on the cooperating elements and the frictional wear occurring between them [2, 3, 8]. As the authors note, dynamic simulations require significant computational effort to run a simulation with a total duration of several seconds of cooperation between the friction elements [3].

Temperature has a fundamental influence on the course of physical phenomena occurring in the components of the braking system. The increase in temperature, combined with the phenomenon of thermal expansion, may lead to the deformation of the friction surfaces of the disc or drum. This, in turn, can result in damage to the braking system components, posing a potential threat. Additionally, it determines the tribological phenomena occurring on the friction surfaces and thus affects the value of the friction coefficient. Therefore, the issues related to the transfer of heat generated in the executive elements of the vehicle braking system, i.e. the heating of the brake disc surface as a result of friction, with simultaneous convective flow of cooling

air, heat radiated by the disc and the process of heat transfer to the suspension components, are so important. Boundary conditions are an important issue in this analysis. Thermal phenomena, as non-linear phenomena, increase the degree of complexity of the studied phenomenon. In the literature, apart from the analysis of deformations and the analysis of the heat flux flow between the brake disc and the brake linings, one can also find the analysis of the impact of heat flow on the elements that are part of the braking system, such as connecting bolts [19, 27]. A general review of simulation methods is presented extensively in this paper [25].

4. Boundary conditions

In heat transfer, both in steady and unsteady states, there are basically three types of boundary conditions. These phenomena have been very well described and are currently also used to describe thermal phenomena not only in the case of cooperation of friction elements but also to describe processes, e.g. energy industry simulations [10, 13, 17].

Boundary conditions of the I type occur when the heat exchange on the surface of the examined area is so intense that the surface of the object immediately assumes the temperature of the environment. This is approximately the case when the tested object has a low thermal conductivity λ_m , and the heat exchange on the surface is very intense. The Biot number characterizes these properties $Bi = \alpha l / \lambda_m \rightarrow \infty$. Then, the body surface temperature $T(x, \tau)$ assumes the temperature of the environment and remains constant throughout the cooling or heating period [1, 11, 13].

$$T_{(x,\tau)}|_{x=0} = T_{ot} \quad (1)$$

Boundary conditions of the II type kind occur when the heat flux q on the heat exchange surface is constant or given by the function [12, 13]:

$$q = -\lambda_m \frac{\partial T}{\partial x} \quad (2)$$

in this case, the body temperature at the surface is unknown.

Boundary conditions of the III type kind occur most often in practice, they consist in the fact that the heat flux exchanged on the surface of the body is proportional to the temperature difference; surface of the body and the medium that surrounds the surface [12, 13]:

$$-\lambda_m \frac{\partial T}{\partial x} \Big|_{x=0} = \alpha (T_{x=0} - T_{ot}) \quad (3)$$

where: T_{ot} – ambient temperature, λ_m – thermal conductivity of the material, α – heat transfer coefficient.

Figure 1 presents a graphical interpretation of the presented boundary conditions.

The literature [1] also indicates boundary conditions of the IV type – they occur when two solid centers exchange heat through contact (Fig. 2). Conditions of this type occur in the case of cooperation of internal combustion engine elements and are used for example, in the case of modeling a cast iron insert under the first sealing ring in the piston. You can then save [12]:

$$-\lambda_1 \frac{\partial T_1}{\partial x_1} \Big|_{x=x_p} = \lambda_2 \frac{\partial T_2}{\partial x_2} \Big|_{x=x_p} \quad (4)$$

where: λ_1 – thermal conductivity of the material (1), λ_2 – thermal conductivity of the material (2).

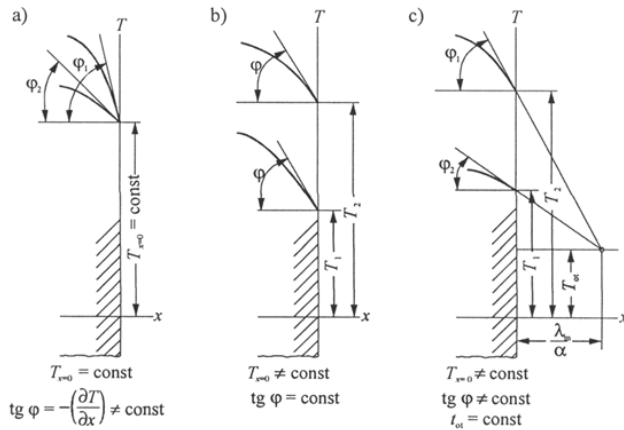


Fig. 1. Graphical interpretation of boundary conditions. Boundary conditions a) I type, b) II type, c) III type [12]

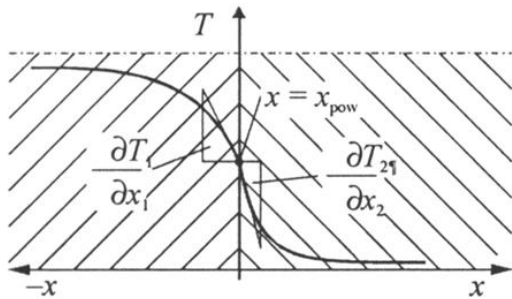


Fig. 2. Graphical interpretation of type IV boundary conditions [12]

5. Unstandable temperature

With regard to changes in the thermal state of the brakes, a single vehicle braking can be divided into two characteristic phases [26]:

- short-term, intense heat impulse
- long-term cooling phase of the brakes after braking.

The heat flux generated in the first phase of braking is many times greater than the heat flux discharged to the environment in the second phase. The first phase is characterized by large temperature gradients in the friction pairs of the brake, and this is of fundamental importance. On the other hand, the outflow of heat to the environment plays an important role in the analysis of long-term or repeated braking cycles, and in the case of single, intensive braking, it is relatively insignificant [26].

The temperature distribution in the friction elements is strictly dependent on the course of the braking process. There are three basic types of braking [26]:

- one-time (short-term until the vehicle stops)
- multiple (repeated at regular intervals)
- continuous, long-lasting (e.g. going downhill).

During single braking, a rapid increase in the temperature of the friction surface of the disc is characteristic, which reaches its maximum values on average in the temperature range 250–300°C. In addition, large temperature gradients are observed in a thin layer of material near the surface. In disc brakes, the distribution of temperatures around the circumference of the friction surface of the

brake is not uniform. During multiple braking, there is an effect of cumulating thermal loads from individual braking, as long as the time between these braking is not too long. The temperature of the friction surface shows large fluctuations in each successive braking. On the other hand, the temperature distribution on the outer surface of the cylindrical and frontal hub is characterized by a uniform increase. This is due to the resistance of heat conduction from the area of its dissipation to the hub of the disc. The most unfavorable state of brake operation is prolonged, continuous braking. In this work, the results of temperature measurements of the friction surfaces of the disc brakes of the Mercedes-Benz 300D W124 car during 21 minutes were used – descent from the Stilfer Pass (covering an average of 48 braking). After 14 minutes on the descent, the maximum temperature of the friction surface of the brake discs was set at 650°C [26].

In addition to frictional wear, the variable temperature field in the brake disc contributes to the formation of cracks and deformations. Their source is high compressive stresses on the friction surface, caused by a large temperature gradient at the surface, which is directed outwards. Compressive stresses cannot initiate the observed cracks, but they can easily cause plastic flow of the material at elevated temperatures, which, after the thermal stresses disappear, leave tensile residual stresses on the friction surface. Tensile stresses can induce thermal cracking, either by cracking non-metallic inclusions or graphite on the surface of the material or by a low-cycle fatigue process with repeated frictional heating cycles. The unsteady temperature field combined with the phenomenon of thermal expansion causes thermal deformation of the brake disc. There are two unfavorable aspects of these deformations. The first is strong thermal stresses arising in these elements, and the second – is temporary disturbances in the functioning of the braking system. The deformation of the disc introduces an uneven distribution of normal pressures on the friction surface and, in extreme cases, a reduction in the contact area. This has the following adverse effects. Firstly, there are local, strong thermal loads on the friction surface, causing intensive, uneven wear. Secondly, there is a decrease in the effectiveness of the brakes resulting from the non-linear dependence of the friction force on the unit pressures [26].

6. Modeling of thermal conductivity in vehicle brakes

The braking process of a car is inherently unsteady, which makes the issue of unsteady heat transfer in the brakes analyzed. The fundamental problem from the point of view of the phenomena and the possibility of solving the problem is the phenomena of heat conduction in the thermal vapors of the brake. In the literature, the phenomenon of conduction, i.e. the phenomenon of heat transfer by conduction (which is very important in the case of contact of friction elements) is described in two ways. In the cylindrical coordinate description of the axial symmetry problem, the following equation (5) describes unstable heat conduction in anybody [18, 20, 21]. The second described in the most recent works is the so-called Galerkin's method [15]. Using Galerkin's method, unsteady heat can be written in matrix form using finite elements.

$$\rho \cdot c_p \cdot \frac{\partial T}{\partial t} = \frac{1}{r} \cdot \left[\frac{\partial}{\partial r} \left(r \cdot \lambda \cdot \frac{\partial T}{\partial r} \right) + \frac{\partial}{\partial \phi} \left(\frac{1}{r} \cdot \lambda \cdot \frac{\partial T}{\partial \phi} \right) + \frac{\partial}{\partial z} \left(r \cdot \lambda \cdot \frac{\partial T}{\partial z} \right) \right] \quad (5)$$

where: ρ – density, r – radial coordinate in the cylindrical system, ϕ – angular coordinate in the cylindrical system, z – angular coordinate in the cylindrical system.

The density of the heat flux emitted on the friction surfaces depends on the coefficient of friction, unit pressures p and the sliding speed V .

$$q = \mu \cdot p \cdot V \quad (6)$$

The time course of the velocity V results from the course of the braking process. It is a function of the braking forces and motion resistance (air resistance, rolling resistance, hills, etc.) and also depends on the phenomena occurring at the contact point between the wheel and the road surface (wheel slip). After determining the time course of the heat flux density q emitted on the friction surfaces, its division into the brake disc and the friction lining (pad) should be taken into account. The most simplified method of analysis assumes the omission of heat penetration into the friction material due to the low thermal conductivity of this material. The material of the friction lining absorbs only a few percent of the heat released. The second method assumes that the heat is distributed to both bodies in proportions equal to their penetration coefficients [13, 26].

7. The phenomenon of friction at the interface between the brake disc and the pad

At the contact between the friction elements of the brake disc and the brake pad, a heat flux q is generated with a value that varies in time (τ), described by the relationship:

$$q(\tau) = N(\tau) \cdot \mu(\tau) \cdot v(\tau) \quad (7)$$

$$[W] = [N] \cdot [-] \cdot \left[\frac{m}{s} \right] = \left[\frac{J}{s} \right] = [W]$$

where: $N(\tau)$ – time-varying pressure of the pad on the disc; This course, in accordance with observations, looks as shown in Fig. 3.

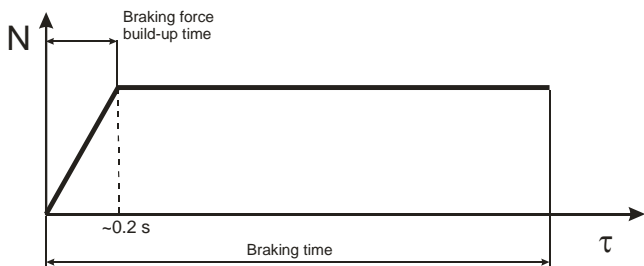


Fig. 3. The course of the pressure force on the brake pad

The pressure force is distributed over the surface of the pad and disc and depends on the contact surface area. Hence the unit pressure $q_i(\tau)$ is:

$$q_i = \frac{q(\tau)}{A} \left[\frac{W}{m^2} \right] \quad (8)$$

where: $q(\tau)$ – total heat flux at the contact surface of the block [W], A – contact area [m²].

The pressure of the pad on the disc is uneven over the contact length along its symmetry axis and depends on the distance of the support point from the contact plane.

Another parameter on which the heat flux $q(\tau)$ depends is the friction coefficient of the pad-disc pair μ . It is assumed that it depends primarily on the speed and material that creates the friction pair. Designers are looking for composites that guarantee a constant value of the friction coefficient as a function of speed. This avoids the impact effect in the final phase of braking (sudden increase in braking force). Braking speed – it is assumed that it decreases evenly from the initial braking value to stop. Most often, a constant braking deceleration is assumed, in accordance with UNECE Regulation R13, equal to $a_b = 5.8 \text{ m/s}^2$.

The potential energy of friction pairs, in accordance with the laws of physics, penetrates the surface of the disc and pad. This flux is divided in proportion to the heat transfer capacity (type II boundary conditions).

$$\frac{q_1}{q_2} = \frac{\lambda_1 \frac{\partial T_1}{\partial x_1}}{\lambda_2 \frac{\partial T_2}{\partial x_2}} \quad (9)$$

where: 1 – applies to the shield, 2 – applies to the block.

Due to the modeling of the heat transfer process, it is important how this process takes place outside the contact of friction pairs – this applies in particular to the brake disc. It is assumed that heat transfer takes place in accordance with type III boundary conditions, i.e. by convection. This process is characterized by two criterion numbers: the Bi (Biot) number and the Fo (Fourier) number. Biot number:

$$Bi = \frac{\alpha \cdot h}{\lambda} \quad (10)$$

characterizes the penetration of heat into the material, where: α – heat transfer coefficient on the surface, h – depth at which the temperature is analyzed, λ – thermal conductivity coefficient of the material. Fourier number:

$$Fo = \frac{a \cdot \tau}{h^2} \quad (11)$$

it is characterized by the equalization of temperature within the analyzed temperature field, where: a – temperature compensation coefficient (temperature conduction)

$$a = \frac{\lambda}{c \cdot \rho} \quad (12)$$

where: c – specific heat, ρ – material density, τ – time.

However, in the case of a brake disc, the thermal operating conditions change with each revolution. This can be presented as a dependence of temperature T as a function of time (τ) – Fig. 4.

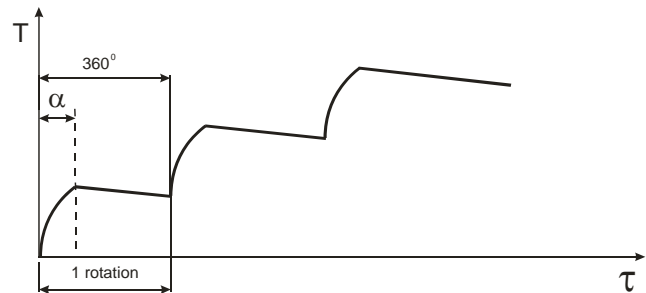


Fig. 4. The course of heating the disc point as a function of the rotation angle

8. Issues of heat exchange with the environment

The issue of heat exchange with the environment includes the process of thermal conduction in friction pairs and modeling of its boundary conditions (heat generation in brakes and heat exchange with the environment).

One of the important problems is the mathematical description of the complex, unsteady heat exchange between the brake surface and the air flowing around it. The heat flux density q exchanged with the environment by convection and by radiation is expressed by the relation [13, 26, 28]:

$$q = q_k + q_{pr} = (\alpha_k + \alpha_{pr}) \cdot (T - T_\infty) \quad (13)$$

$$\alpha = \alpha_k + \alpha_{pr} \quad (14)$$

where: q_k – heat flux density flowing to the environment by convection, q_{pr} – heat flux density exchanged with the environment by radiation, α_k – heat transfer coefficient by convection, α_{pr} – heat transfer coefficient by radiation, α – total heat transfer coefficient, T – brake surface temperature, T_∞ – ambient temperature.

It is difficult to determine the heat transfer coefficient α_k , which is a function of many variables. Its value depends on the physical properties of the air (viscosity, density, thermal conductivity, specific heat), which are functions of temperature and, to a lesser extent, air pressure. However, above all, this coefficient depends on the speed and the way the air flows around the brake (laminar, turbulent). The problem becomes more complex because due to the change in time: vehicle speed, wheel rotational speed, and brake surface temperature, there is an unsteady heat exchange in the vehicle (these values determine the value of the heat transfer coefficient). It is much simpler to determine α_{pr} . According to the Stefan-Boltzmann law, the density of the heat flux radiated by the gray body is expressed by the relationship [13, 17, 26]:

$$q_{pr} = \varepsilon \cdot c_0 \cdot \left[\left(\frac{T}{100} \right)^4 - \left(\frac{T_\infty}{100} \right)^4 \right] \quad (15)$$

Therefore, the following mathematical relationship for the heat transfer coefficient by radiation can be introduced [26]:

$$\alpha_{pr} = \varepsilon \cdot c_0 \cdot \frac{\left(\frac{T}{100} \right)^4 - \left(\frac{T_\infty}{100} \right)^4}{T - T_\infty} \quad (16)$$

where: ε – emissivity for a cast iron disc 0.29–0.30, c_0 – specific heat, T – brake surface temperature, T_∞ – ambient temperature.

At a constant ambient temperature T_∞ , the coefficient α_k is proportional to the third power of the brake surface temperature. The percentage share of radiation in the overall heat exchange between the brakes and the environment is significant only at high temperatures of the friction surfaces of the discs – of the order of 400–800°C. The phenomenon of radiation cannot be omitted in the case of long-term and cyclic braking. Heat exchange with the environment takes place mainly as a result of forced convection – cooling air flows around the brake. The dependence of α_k on temperature is relatively insignificant. For this reason, taking into account these comments, it is justified to assume a linear boundary condition of the third kind for the equation of thermal conductivity in the brake disc [23, 26, 28].

The surface of the disc heats up to high temperatures and has the largest share of the total heat transfer surface. In a disc brake, the brake pads detach the aerodynamic boundary layer, thereby significantly increasing heat transfer compared to discs where movement is caused by layer friction. The empirical coefficient α_k of heat exchange with the environment by convection is presented in relation (17) [13, 26, 28]:

$$\alpha_k = \frac{0.076}{(2\pi)^{0.2}} \lambda_p \cdot r_{sr}^{0.6} \cdot \left(\frac{\omega}{v_p} \right)^{0.8} \quad (17)$$

where: r_{sr} – average friction radius of the brake disc [m], λ_p – thermal conductivity coefficient [W/mK], ω – angular velocity of the braked wheel [rad/s], v_p – coefficient of kinematic viscosity of air [m²/s].

The density of the heat flux flowing into the disc during braking q' is many times greater than the density of the flux flowing out to the environment. This means that during intensive, short-term braking, brake cooling contributes little to the energy balance. Heat flow plays an important role in the analysis of long-term or repeated braking cycles [19, 26, 27].

The analysis shows that the phenomena accompanying the braking process in a vehicle are very complex, and an attempt to model them may turn out to be complicated. In this work, the modeling of the heat exchange phenomenon was limited to the study of the behavior of the brake disc subjected to long-term exposure to high temperature. The cooling of the brake disc by flowing air was not simulated, nor was heat conduction to the suspension components taken into account. However, in the literature [7, 14, 26] one can find descriptions of the procedure for modeling heat transfer in a car brake, which include, among others, empirically determined relationships describing heat dissipation to the environment.

9. Brake disc analysis

Brake discs, like brake drums, are mounted on the wheel hubs. In most applications, discs are made of gray cast iron or cast steel. Due to the smaller surface of the friction linings, the clamping forces in the brake disc are greater than in the case of the drum. This contributes to greater heat generation and faster wear of disc brake pads in comparison to drum brake linings. When driving, air flows around the brake disc and cools it well. A distinction is made between solid and so-called disc brakes. Ventilated discs can be washed with air from the outside or inside (Fig. 5). Ventilated discs have a higher heat capacity due to their greater mass and cool down faster due to the radially arranged channels through which the air flows [9].

In the conducted tests, a ventilated brake disc was selected for the strength analysis. The damage to this disc consisted in its significant deformation, which was confirmed by axial runout measurements. For comparison, measurements of the axial runout values of a similar wheel that was properly worn were also carried out. As a result of the measurements carried out, even after such a long period of use, did not exceed the permissible axial runout value of 0.06 mm, as specified by the vehicle manufacturer. The basis for replacing this disc was only to reduce its thickness

by 5 mm), which is considered normal wear resulting from the operation of the vehicle.

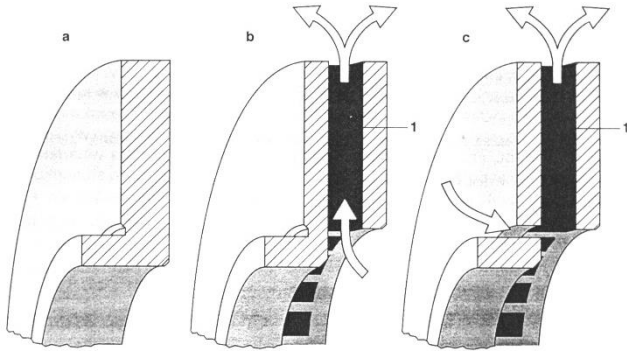


Fig. 5. Types of brake discs [2], where: a – solid brake disc, b – internally ventilated brake disc, c – externally and internally ventilated brake disc, 1 – cooling duct

9.1. External evaluation

Figure 6 shows a general view of the brake disc worn "properly" as a result of the operation, while Fig. 7 shows a deformed brake disc after a very short period of operation, which was the subject of further analysis. After the axial runout measurements and preliminary inspection, the deformed disc was cut along its diameter to examine the disc material's structure on the cross-section and to facilitate the preparation of the computational model.

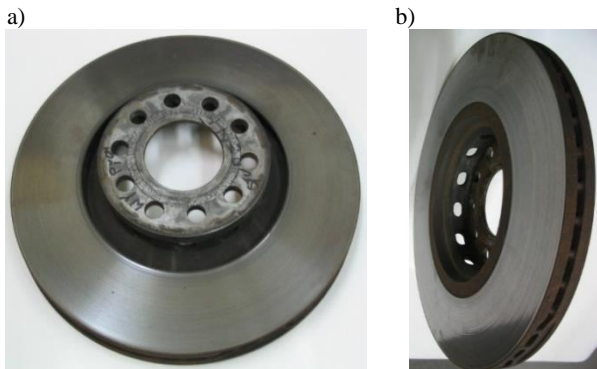


Fig. 6. Brake disc with proper exploitation wear: a) external side, b) internal side

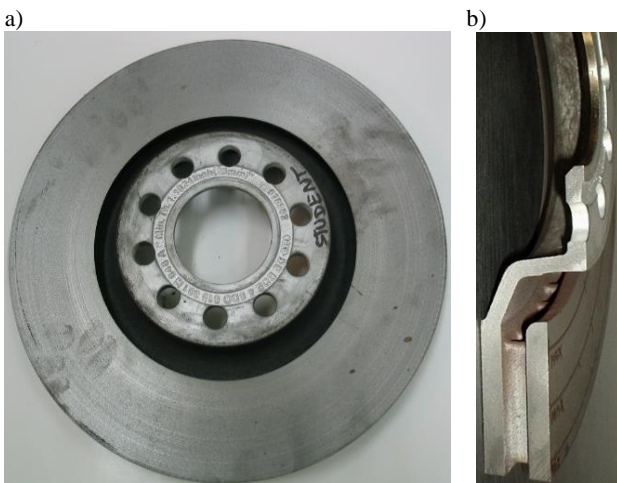


Fig. 7. Deformed brake disc: a) general view, b) cross-section of the disc

9.2. Comparative disc analysis

The main purpose of the comparative analysis of the two discs was to confirm the incorrect wear of one of them. In relation to the limit of permissible radial runout of 0.06 mm specified by the vehicle manufacturer, the disc worn as a result of normal operation did not show shape deviations on the friction surfaces. This assessment does not take into account the effect of roughness. This shield came from a similar vehicle and differed only in the use of additional ventilation channels in the vicinity of the shield mounting points. However, the geometric dimensions of both discs were the same.

The measurement of the axial runout of the brake discs was carried out using a dial indicator with an elementary division of 0.01 mm. Three measuring diameters were determined on both discs and then ten measuring points spaced every 36 degrees were determined on each diameter. Measurements were made on both sides of the disc (outer and inner sides). The measurement results obtained for a deformed disc are shown in Fig. 8, 9, and for a worn disc is correctly shown in Fig. 10 and 11.

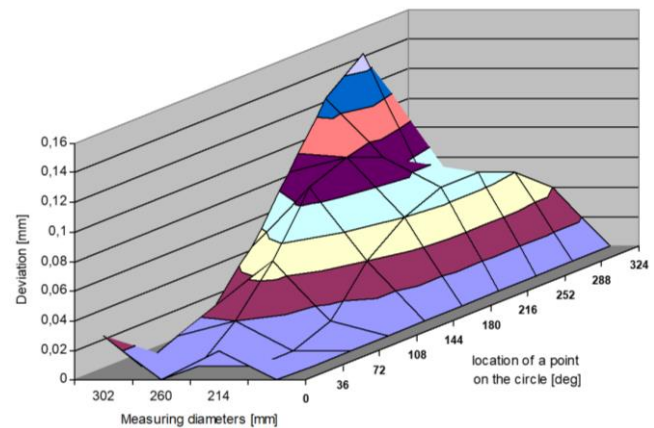


Fig. 8. Measurement results on the "deformed" surface of the brake disc. External page

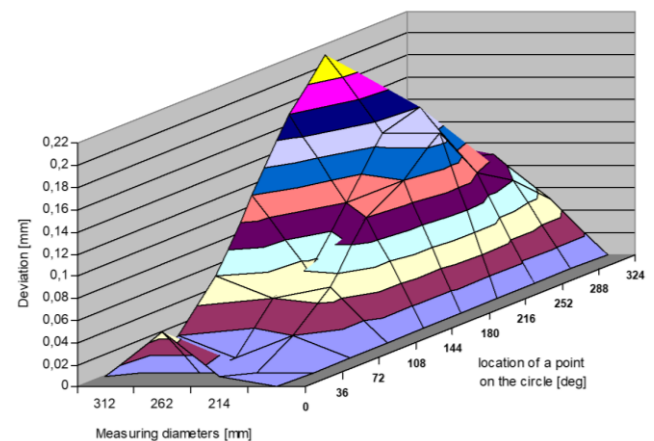


Fig. 9. Measurement results of the "deformed" brake disc surface. Inside page

As a result of the measurements, it was found that on the surface of the "deformed" brake disc, in several measurement points, the permissible values of axial runout spec-

ified by the manufacturer at 0.06 mm were almost three times exceeded. The second disc is properly worn, despite being used for 2 years at a distance of 70,000 km did not exceed the permissible deviation of the shape of the friction surfaces. Taking into account the above conclusions, further analysis was carried out using successively metallographic tests and analyses, as well as FEM calculations and strength analysis.

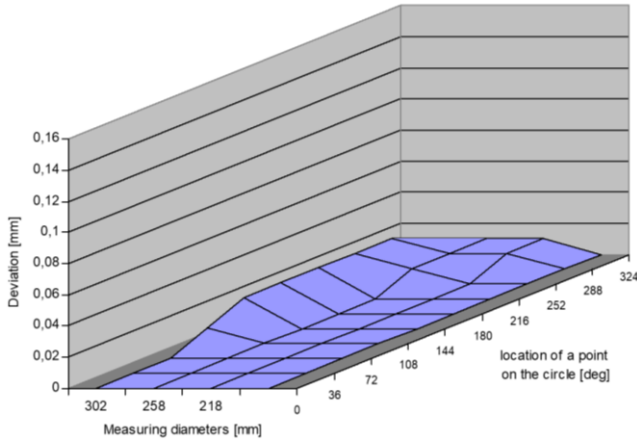


Fig. 10. Results of measurements on the surface of a properly worn brake disc, external side

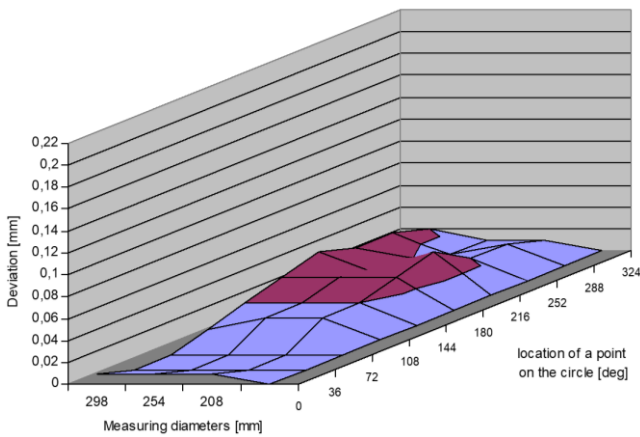


Fig. 11. Results of measurements on the surface of a properly worn brake disc inside

9.3. Shield model

The basic dimensions of the deformed brake disc are listed in Table 4.

Table 4. Basic dimensions of the brake disc

outer diameter [mm]	overall plate thickness [mm]	total height of the shield [mm]	hub hole diameter [mm]	spacing of holes for mounting screws [mm]
321	30	42	68	10 × 112

The geometric model of the analyzed brake disc and the basic technical documentation were made in the CATIA program. Figure 12 shows the view of the geometric model prepared for further analysis.

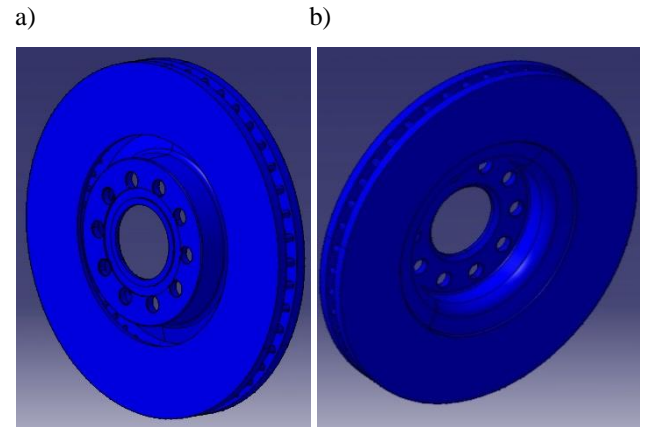


Fig. 12. Geometric model of the brake disc: a) view from the outside, b) view from the inside

10. Numerical analysis of the brake disc

In the last stage of the research, in order to identify and determine the cause of the deformation of the brake disc, a strength analysis was carried out using the Finite Element Method. For this purpose, a simulation of a long-term brake disc load under conditions of high temperature, not exceeding the temperature limit for structural changes of the disc material, was carried out. For this type of cast iron, the limit temperature is approx. 700°C.

When starting the FEM strength analysis of the brake disc, it was expected that the calculation results would confirm the deformation of the brake disc and at least indicate the cause of such a situation. In particular, this concerned the material from which the shield was made. On the basis of metallographic tests, it was found that the disc was not "overheated", i.e. its temperature did not exceed the limit of 700°C. Therefore, it was decided to study its behavior at a long-term temperature slightly lower – 650°C. Due to the fact that it was not physically possible to measure temperatures in real conditions on the object, the data from the measurements included in the work [26] were used. The results of brake disc temperature measurements in the Mercedes-Benz 300D W124 car during the descent from the Stilfer Pass in the Alps were quoted. The strength analysis was carried out using the I-DEAS 10 system.

10.1. Boundary conditions

As boundary conditions in the FEM analysis of the brake disc model, input parameters such as: disc material properties (Table 5), disc heating curve (Table 6), and support conditions (Fig. 13) were adopted.

Table 5. Properties of the brake disc material [1]

	Temperature [°C]							
	20	100	200	300	400	500	600	700
Density [kg/m ³]	7100							
Conductor coefficient heat λ [W/mK]	42	60	51.9	43.3	38.6	34.6	31.1	29.9
Specific heat C_p [J/kg·K]	489	498	517	539	567	584	599	612
Expansion linear factor heat [$\times 10^{-5}$]	1.0				1.3			

On the other hand, for static calculations, i.e. stress and displacement analyses, temperatures in individual nodes, derived from thermal calculations, were additionally set (Fig. 14).

Table 6. Brake disc heating curve [26]

Time [s]	0	25	50	75	100	150
Temperature [°C]	20	62	80	104	196	242
Time [s]	200	250	300	350	400	450
Temperature [°C]	288	331	370	390	430	490
Time [s]	500	550	600	700	800	
Temperature [°C]	580	630	638	640	645	

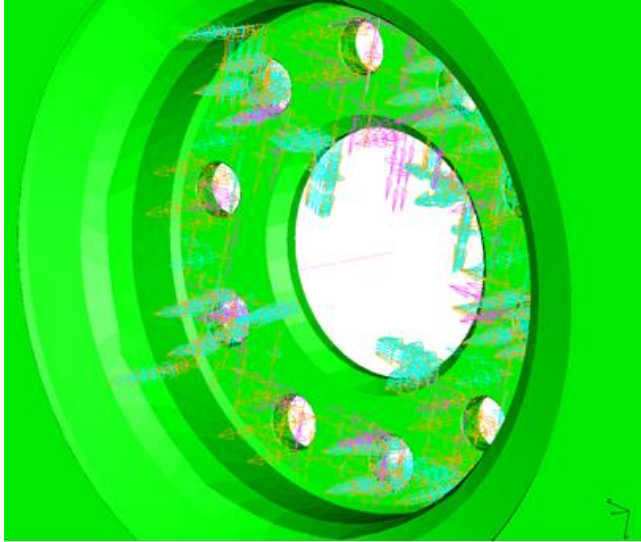


Fig. 13. Support of the brake disc model

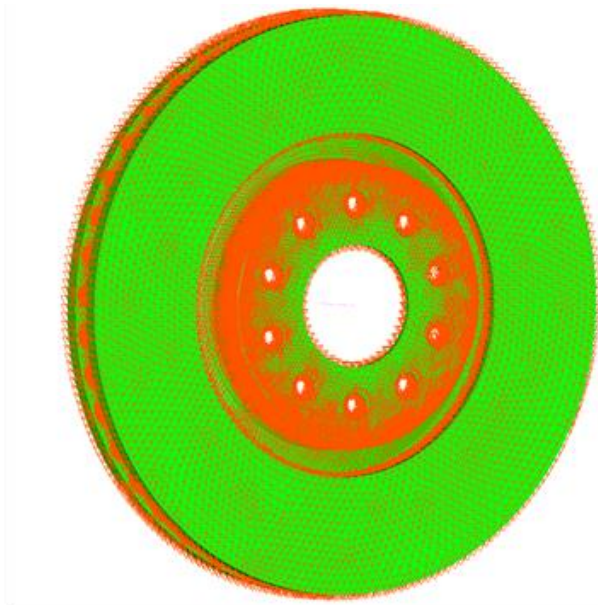


Fig. 14. Set temperatures in individual nodes of the brake disc

10.2. Calculation model

The computational model was created based on the geometrical parameters of the actual brake disc described in the previous chapters and is its faithful reflection.

For the discretization of the geometric model, higher-order volumetric elements of the TETRA 10 type, optimal for thermal analyses, were used (Fig. 15).

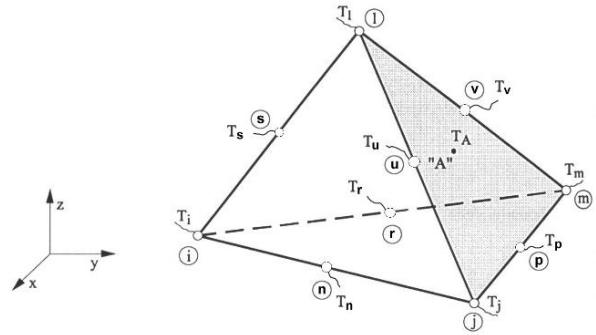


Fig. 15. TETRA 10 finite element [21]

The discrete model of the brake disc contained 68,834 SOLID finite elements and 121,325 nodes. In addition, in order to simulate the process of heat exchange with the environment, two shell grids (SHELL) were created. One necessary to set the heat flux entering the target contained 2710 finite elements. The second coating mesh, necessary to simulate heat transfer, contained 28,206 finite elements and was applied to all surfaces of the brake disc. The process of heat conduction to the disc (simulation of the disc heating process as a result of the friction of the pad-disc assembly) was caused by the temperature gradient – the heating curve. On the other hand, the disc cooling process (cooling in the "free air") was caused by free convection with the heat transfer coefficient $\alpha = 4 \text{ W/m}^2\text{K}$. As indicated in the previous chapters of the work, due to objective reasons, the analysis did not take into account the heat conduction through the disc to the suspension elements and the heat radiated by the heated disc. On the other hand, in the disc cooling process, an important simplification was that the cooling air had equal access to all surfaces of the brake disc. The direction and direction of the gravitational acceleration vector were assumed in accordance with the actual position of the brake disc mounting in the vehicle, i.e. along the X axis and directed downwards – Fig. 16. The ambient temperature was assumed to be 20°C.

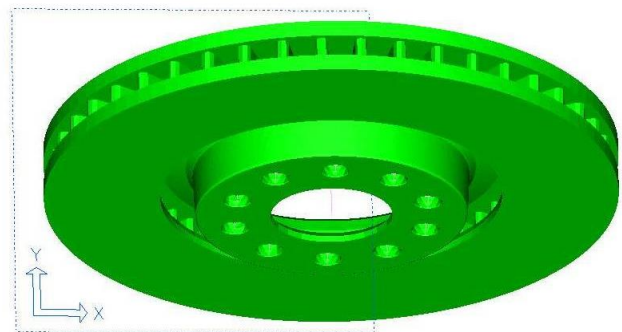


Fig. 16. Orientation of the coordinate system for the shield model

10.3. FEM calculation results

The following figures show the results of FEM calculations of the brake disc. The results include thermal analysis, i.e. the distribution of temperatures on the disc surface after successive time steps, and thus the course of "cooling down" of the brake disc cooled in "free air". The time steps have been selected so as to record clear changes in the behavior of the disc during heating and cooling. In addition,

strength calculations were carried out to obtain the distribution of stresses in the disc and displacements. The measurement results are presented in Table 7 and in Fig. 19 and in Table 8, while in Fig. 18, 19 selected characteristic temperature distributions are presented, and in Fig. 20–23 displacements and stresses are presented.

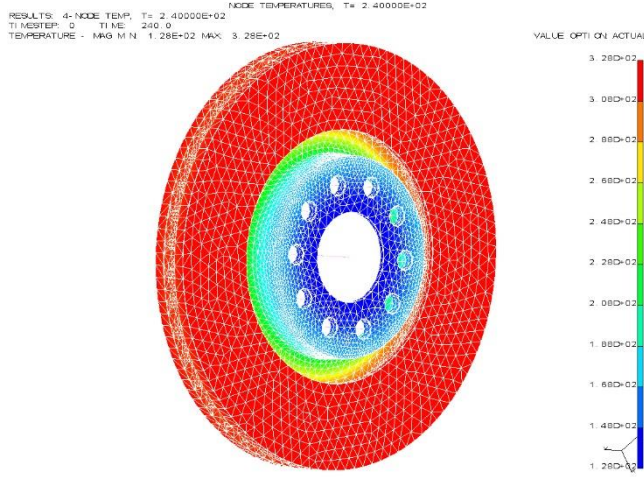


Fig. 17. Temperature distribution [°C] after 240 s for a cast iron disc

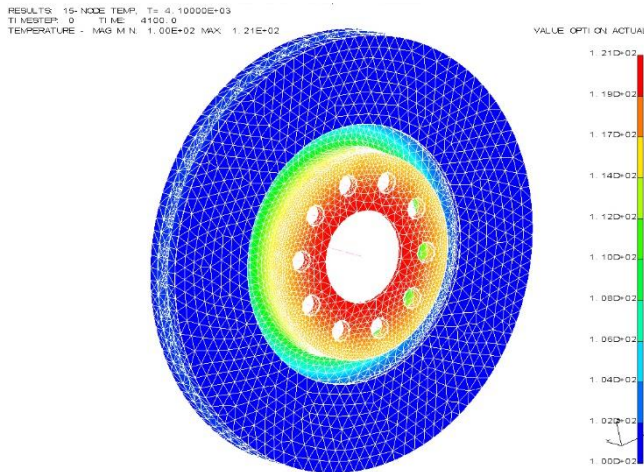


Fig. 18. Temperature distribution [°C] after 4100 s for a cast iron disc

Table 7. Temperature values of the cast iron disc in successive time steps

Time [s]	Temperature max [°C]
0	20
240	328
560	632
800 (end of warm-up)	644
1,500	521
2,400	368
3,600	170
4,100	121

Based on the results of the FEM calculations of the cast-iron brake disc collected in Table 8, it can be concluded that there is deformation of the brake disc. The obtained values are debatable. On the other hand, the values of maxi-

Table 8. Results from the FEM analysis for the cast-iron brake disc

Time [s]	Temperature max [°C]	Stress max according to HMH [MPa]		Displacement [mm]
240	328	97		0.56
560	632	288	$\sigma_x = 115$ $\sigma_y = 90.2$	1.14
800 (end of warm-up)	644	420		1.16
1500	521	430		0.83
2400	368	298		0.54
3600	170	128		0.23
4100	121	85		0.14

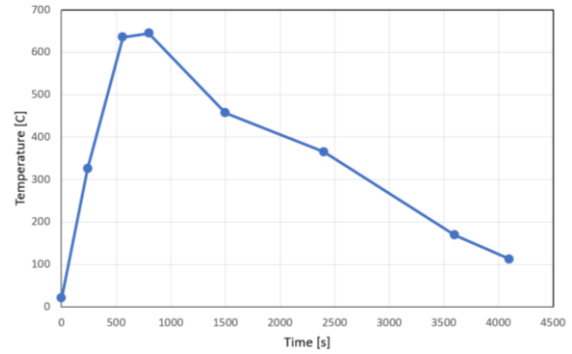


Fig. 19. Heating curve and cast iron disc

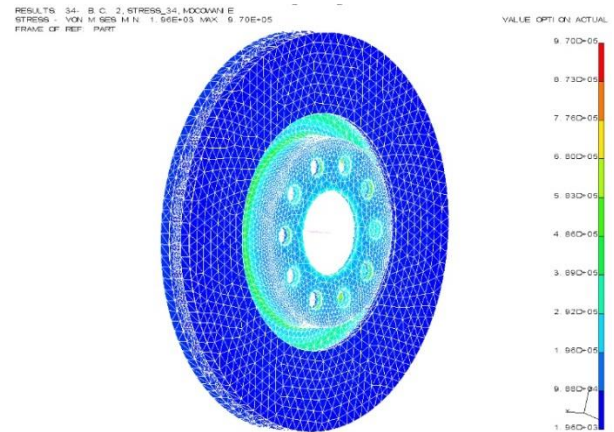


Fig. 20. Equivalent stresses [hPa] according to the HMH hypothesis for 240 s

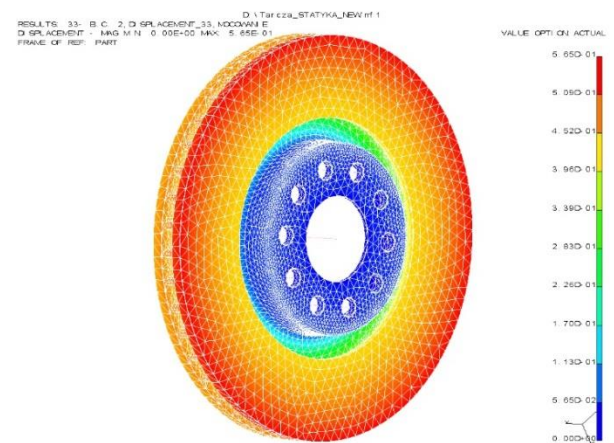


Fig. 21. Displacements [mm] after 240 s

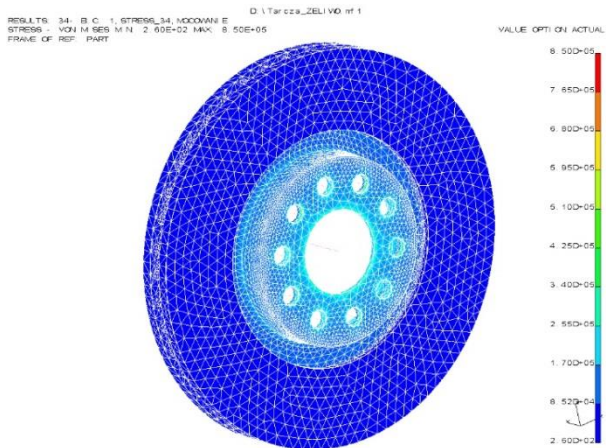


Fig. 22. Equivalent stresses [hPa] according to the HMM hypothesis for the time of 4100 s

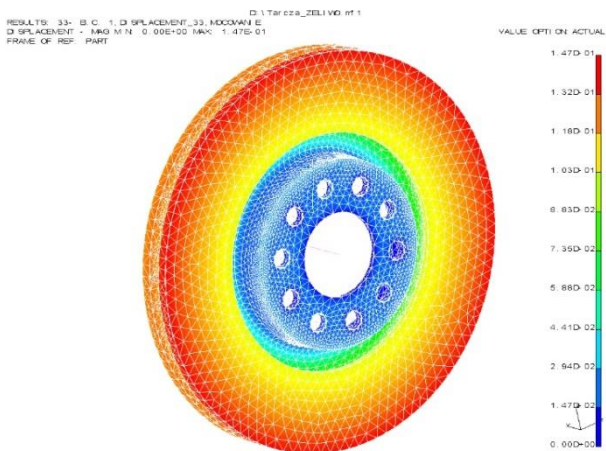


Fig. 23. Displacements [mm] after 4100 s

num stresses in the disc at the highest temperatures and during cooling may raise concern. However, it turns out that the values of these stresses are local and after a more detailed analysis of the entire structure, it can be seen that stresses outside these places are evenly distributed, and their values are at least an order lower than the yield strength of the disc material. However, this statement can be partly explained by the "waving" of the tested brake disc, which means that in the places of stress concentration, microcracks of the material could have formed and caused "deformation" of the disc. The situation is similar with respect to displacements. The values resulting from the FEM analysis are much higher than the values measured in the real object. However, this can be explained by the fact that the heat transfer process in the car brake is much more complicated than included in the numerical model, which has been simplified and does not take into account many aspects that could affect the results of the analysis. This applies, for example, to the method of mounting the disc to the wheel hub and its additional stabilization by the brake caliper, covering a significant part of the friction surfaces of the brake disc.

11. Conclusions

The results of FEM calculations for the cast iron disc confirmed the deformation of the brake disc. This phenom-

enon had a similar character and course in the FEM analysis as in the real object. However, some discrepancies occur if the values of real measurements and computer simulations are taken into account. At the maximum value of the displacement during the measurements of the axial runout of the brake disc, a displacement of 0.22 mm was obtained. On the other hand, in the FEM results, the value of the maximum displacement was recorded when the disc reached the maximum temperature of 1.16 mm. It follows from the above that the differences in displacement are quite significant. However, the reason for these differences may be the simplifications of the numerical model, which were indicated in the previous chapters. The situation is similar in the case of the obtained stress results, the maximum values of which may be disturbing, as they exceed the yield point value for cast iron almost three times. However, more important than local stress concentrations – which may cause microcracks and, as a result, disc deformation – is the global stress distribution, which is acceptable and does not raise concerns. However, only on the basis of the analysis of the results of numerical calculations, it is impossible to answer the question of why the dial was bent.

12. Directions for further work

The main purpose of the work was to identify the phenomena and behavior of the brake disc and to try to reproduce them, as well as to signal the complexity of these issues.

Unfortunately, in the work, it was not possible to obtain a clear answer to the question about the direct cause of the brake disc damage. However, a good starting point for further work on these issues are the tests carried out and calculations that can be used for the test, with the use of which an attempt can be made to change the geometry of the tested brake disc and additionally use other materials.

Despite many advantages and progress in the construction of brakes other than friction brakes (e.g. electric electromagnetic brakes), friction brakes seem to be irreplaceable. Compared to other solutions, they are light, small, and cheap, hence their safe use in cars, trains, airplanes, and in various industrial devices. In the foreseeable future, no significant changes in the principles of brake operation or fundamental changes in the design features of friction elements and brake drives are to be expected. As the numerical analysis has shown, it is advisable to introduce more and more different, newer, and more specialized friction materials for linings as well as friction races of brakes. Since in friction brakes, the kinetic energy of moving vehicles or machines is converted mainly into heat, the following problems will remain valid in the further stages of development of these brakes: thermal resistance of friction materials, heat capacity and ability to dissipate heat, and thermoelastic stability of friction system elements. Other inseparable problems of almost every friction node are: stabilization of the friction coefficient, minimization of wear, and noise reduction. Therefore, the starting point for further work should be an attempt to replace the traditional material (cast iron) with another alternative material. This was initiated by carrying out FEM calculations for a composite target.

Nomenclature

c_0	specific heat [J/kgK]	V	sliding speed [m/s]
c_p	specific heat [J/kgK]	z	angular coordinate in the cylindrical system
FEM	Finite Element Method	α	heat transfer coefficient [W/m ² K]
HMH	Huber-Mises-Hencky	α_k	heat transfer coefficient by convection [W/m ² K]
p	pressure [Pa]	α_{pr}	heat transfer coefficient by radiation [W/m ² K]
q	heat flux density [W/m ²]	ε	emissivity for a cast iron disc [-]
q_k	heat flux density flowing [W/m ²]	λ_m	thermal conductivity of material [W/mK]
q_{pr}	heat flux density exchanged with the environment by radiation [W/m ²]	λ_p	thermal conductivity coefficient [W/mK]
r	radial coordinate in the cylindrical system	$\lambda_{1,2}$	thermal conductivity of material [W/mK]
r_{sr}	average friction radius of the brake disc [m]	μ	friction coefficient [-]
T	brake surface temperature [K]	ν_p	coefficient of kinematic viscosity of air [m ² /s]
T_{ot}	ambient temperature [K]	ρ	density [kg/m ³]
T_{∞}	ambient temperature [K]	φ	angular coordinate in the cylindrical system
		ω	angular velocity of the braked wheel [rad/s]

Bibliography

- [1] Automotive engineer handbook. Elements and materials. WKŁ Warsaw 1990.
- [2] Baranowski P, Damaziak K, Małachowski J. Brake system studies using numerical methods. *Eksplot Niezawodn.* 2013;15(4):337-342.
- [3] Baranowski P, Damziak K, Malachowski J, Mazurkiewicz L, Kastek M, Piatkowski T et al. Experimental and numerical study of thermo-mechanical processes occurring on brake pad lining surfaces. *WIT Trans Eng Sci.* 2011;71(X): 15-24. <https://doi.org/10.2495/SECM110021>
- [4] Belhocine A, Abdullah OI. Thermomechanical model for the analysis of disc brake using the finite element method in frictional contact. *Multiscale Science and Engineering.* 2020;2:27-41. <https://doi.org/10.1007/s42493-020-00033-6>
- [5] Chen Y, Gao F, Fu R, Su L, Han X et al. Braking-experimental study on the relationship between friction material type and brake disc temperature. *Ind Lubr Tribol.* 2022; 74(8):975-984. <https://doi.org/10.1108/ILT-03-2022-0107>
- [6] Djafri M, Bouchetara M, Busch C, Weber S. Effects of humidity and corrosion on the tribological behaviour of the brake disc materials. *Wear.* 2014;321:8-15. <https://doi.org/10.1016/j.wear.2014.09.006>
- [7] Gao CH, Lin XZ. Transient temperature field analysis of a brake in a non-axisymmetric three-dimensional model. *J Mater Process Tech.* 2002;129:513-517. [https://doi.org/10.1016/S0924-0136\(02\)00622-2](https://doi.org/10.1016/S0924-0136(02)00622-2)
- [8] Guru Murthy Nathi, Charyulu TN, Gowtham K, Satish Reddy P. Coupled structural/thermal analysis of disc brake. *International Journal of Research in Engineering and Technology.* 2012;1(4):539-553. <https://doi.org/10.15623/ijret.2012.0104004>
- [9] Informator Techniczny Bosch. Conventional brake systems of passenger cars. 2001 Edition.
- [10] Jin P, Xue Y, Chen B, Wang L. An analytical solution of temperature near nuclear waste canister under three-dimensional heat transfer condition progress in nuclear energy. *Prog Nucl Energ.* 2021;143:104051. <https://doi.org/10.1016/j.pnucene.2021.104051>
- [11] Kirillov PL, Ninokata H. Heat transfer in nuclear thermal hydraulics. Thermal-hydraulics of water-cooled nuclear reactors. Woodhead Publishing. 2017:357-492. <https://doi.org/10.1016/C2015-0-00235-0>
- [12] Kwaśniewski S, Sroka ZJ, Zabłocki W. Thermal load modeling in internal combustion engine components. Publishing House of Wrocław University of Science and Technology. Wrocław 1999.
- [13] Lu Q. A Finite Element approach for nonlinear, transient heat conduction problems with convection, radiation, or contact boundary conditions. *Ann Nucl Energy.* 2023;193: 110009. <https://doi.org/10.1016/j.anucene.2023.110009>
- [14] Mackin TJ, Noe SC, Ball KJ, Bedell BC, Bim-Merle DP et al. Thermal cracking in disc brakes. *Eng Fail Anal.* 2002; 9(1):63-76. [https://doi.org/10.1016/S1350-6307\(00\)00037-6](https://doi.org/10.1016/S1350-6307(00)00037-6)
- [15] Muthu Visakan M, Mahesh Kumar U, Sivadasan VK. Review on braking system in railways. *International Research Journal of Engineering and Technology.* 2021; 8(7):2333-2339. <https://www.irjet.net/archives/V8/i7/IRJET-V8I7411.pdf>
- [16] Osenin YI, Krivosheya DS, Osenin YY, Chesnokov AV. Disc brake design with carbon friction material. *J Frict Wear+.* 2023;44:13-17. <https://doi.org/10.3103/S1068366623010087>
- [17] Pinca-Bretotean C, Bhandari R, Sharma C, Dhakad SK, Cosmin P, Sharma AK. An investigation of thermal behavior of brake disk pad assembly with Ansys. *Mater Today-Proc.* 2021;47(10):2322-2328. <https://doi.org/10.1016/j.matpr.2021.04.296>
- [18] Popescu FD, Radu SM, Andraş A, Brînaş I, Budilică DI, Popescu V. Comparative analysis of mine shaft hoisting systems brake temperature using finite element analysis (FEA). *Materials.* 2022;15(9):3363. <https://doi.org/10.3390/ma15093363>
- [19] Qu J, Wang W, Wang B, Li G, Jiao B. Analysis of the axial load of bolts of wheel-mounted brake discs of high-speed trains. *Eng Fail Anal.* 2022;137:106250. <https://doi.org/10.1016/j.engfailanal.2022.106250>
- [20] Riva G, Varriale F, Wahlström J. A Finite Element Analysis (FEA) approach to simulate the coefficient of friction of a brake system starting from material friction characterization. *Friction.* 2021;9(1):191-200. <https://doi.org/10.1007/s40544-020-0397-9>
- [21] Rusiński E, Czmochoński J, Smolnicki T. Advanced Finite Element Method in load-bearing structures. Publishing House of Wrocław University of Science and Technology. Wrocław 2000.
- [22] Ścieszka S. Friction brakes. Material, design, and tribological aspects. Library of Maintenance Problems. Gliwice 1998.
- [23] Tauviqirrahman M, Muchammad M, Setiazi T, Setiyana B, Jamari J. Analysis of the effect of ventilation hole angle and material variation on thermal behavior for car disc brakes using the finite element method. *Results in Engineering.*

- 2023;17:100844.
<https://doi.org/10.1016/j.rineng.2022.100844>
- [24] Tripathi VK, Saini R, Joshi UK. Design and analysis of ventilated disc brake by using different materials: a review. International Journal for Research in Applied Science and Engineering Technology. 2023;11:627-631.
<https://doi.org/10.22214/ijraset.2023.55181>
- [25] Usmani D, Mohan R, Mewada CS, Goga G. A comprehensive literature review on the recent advances in braking systems technology using FEA. J Phys Conf Ser. 2023;2484.
<https://doi.org/10.1088/1742-6596/2484/1/012034>
- [26] Walczak S, Wolff A. Theoretical and experimental analysis of heat exchange in automotive brakes. Doctoral Dissertation. Warsaw University of Technology, Faculty of Automotive and Construction Machinery Engineering. Warsaw 2001.
- [27] Wang Q, Wang Z, Mo J, Zhang L. Nonlinear behaviors of the disc brake system under the effect of wheel-rail adhesion. Tribol Int. 2022;165:107263.
<https://doi.org/10.1016/j.triboint.2021.107263>
- [28] Yin J, Lu C, Mo J. Comprehensive modeling strategy for thermomechanical tribological behavior analysis of railway vehicle disc brake system. Friction. 2024;12:74-94.
<https://doi.org/10.1007/s40544-023-0735-9>
- [29] Zemlik M, Dziubek M, Pyka D., Konat Ł, Grygier D. Case study of accelerated wear of brake discs made of grey cast iron characterized by increased thermal stability. Combustion Engines. 2022;190(3):45-49.
<https://doi.org/10.19206/CE-146698>

Prof. Wojciech Ambroszko, DEng. – Faculty of Mechanical Engineering, Wrocław University of Science and Technology, Poland.
 e-mail: wojciech.ambroszko@pwr.edu.pl



Prof. Włodzimierz Dudziński, DSc., DEng. – Collegium Witelona Legnica, Poland.
 e-mail: wlodzimierz.dudzinski@pwr.edu.pl



Sławomir Walczak, MEng. – Graduate student, Wrocław University of Science and Technology, Poland.
 e-mail: sławomir.walczak.oca@outlook.com

